Molecular Photography in the Undergraduate Laboratory: Identification of Functional Groups Using Scanning Tunneling Microscopy

Leanna C. Giancarlo, Hongbin Fang, Luis Avila, Leonard W. Fine, and George W. Flynn*
Department of Chemistry, Columbia University, New York, NY 10027; **flynn@chem.columbia.edu*

In little more than a decade, the scanning tunneling microscope (STM) has proved to be a powerful revolutionary research tool and the first generation of a family of scanning probe microscopes (SPMs) that can be used to study bare surfaces as well as atoms and molecules adsorbed on surfaces. With equal speed SPM principles and practices are finding a place in undergraduate and high school laboratory curricula as a demonstration of state-of-the-art surface analytical techniques. The introduction of SPM to students at this level derives from the relative ease of use of the instrumentation and the quick visual images obtained during the experiments. Several papers in this *Journal* have demonstrated the types of laboratory experiments that can be conducted using these microscopes (*1*, *2*). Generally, these experiments emphasize collection of bare surface topographies and recognition of morphological surface changes due to reaction.

The investigation described below adds to the ideas enunciated in these previous papers by stressing the role of SPM as an atomic or molecular camera. Here, however, the students are asked not only to take "snapshots" of the atoms of bare surfaces but also to identify chemically significant portions (functional groups) of molecular adsorbates placed upon those surfaces. Functional group characterization by SPM is more pictorial and appears more concrete than the traditional "fingerprint" methods of identification used in electronic and vibrational spectroscopies. This empowers students by allowing them to obtain visual evidence for concepts that to this point in their studies may have seemed abstract. For example, students can see the effects of hydrogen bonding in molecular thin film formation. In addition, theoretical methods are introduced here, underscoring the complementary relationship between theoretical predictions and experimentally measured results. Calculations using commercially available software routines enable students to reflect critically on the transfer to a graphical form of the ideas taught in lecture (specifically, ab initio and semiempirical methods in quantum mechanics).

We describe a scanning tunneling microscope investigation of bare graphite and 11-bromoundecanol adsorbed on graphite suitable for undergraduate physical chemistry laboratory students. In addition to collecting substrate (surface) and adsorbate (molecule) images, students use Spartan, a generally accessible computational chemistry software package, to calculate the shapes of the frontier molecular orbitals of a structurally similar but shorter (and thus computationally more efficient) brominated alcohol to compare with their collected STM images. This calculation drives home the fact that the areas of high tunneling current recorded by the STM actually reflect regions of greater electron density of states rather than the position of individual atoms.

The Scanning Tunneling Microscope

The STM is one in a family of instruments (SPMs) that are gaining increasing importance in surface analysis. Developed in 1981 by Gerd Binnig and Heinrich Rohrer at IBM Zurich, the STM allows for the identification not only of single atoms on a conductive surface (or substrate) but also of molecules adsorbed on those surfaces (*3*). The STM works by raster scanning a sharp metal tip over a metal or semiconductor substrate (*4*). (An excellent description of raster scanning in SPM is given in ref *2*.) A bias voltage applied between the tip and the conductive sample induces electrons to "jump" (tunnel) between the two when the tip is in proximity to the sample (from a few to tens of angstroms separation). The remarkable atomic resolution of the STM derives from the fact that the tunneling current is a very rapidly decaying exponential function of the distance between the tip and sample:

$$I \approx V \exp(-Cd) \qquad (1)$$

where I is the tunneling current, V is the applied bias voltage, C is a constant (which includes the potential barriers, known as work functions, for the tip and the substrate; C typically has a value in the range of a few reciprocal angstroms), and d is the tip-to-sample distance.

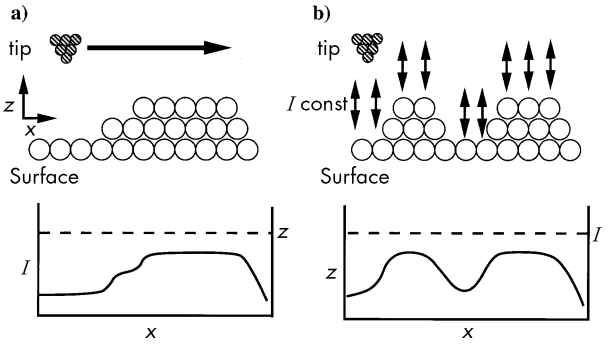

Figure 1. Schematic representations of (a) constant-height and (b) constant-current modes of STM operation. For constant height, the tip is held at a fixed distance from the surface in the z direction while it is raster-scanned in the x (shown) and y (not shown) plane. The collected images reflect an electron tunneling current map (left ordinate) for x,y positions for this fixed height above the conductive surface (right ordinate). In constant-current mode, the tip is moved up and down in the z direction to match the measured tunneling current to that set by the user. This procedure is repeated at each x,y position, producing a topographic map of the surface consisting of the height of the tip (left ordinate) required to equalize the measured and set tunneling currents (right ordinate).

As shown in Figure 1, the STM has two modes of operation: constant height (a) and constant current (b). In the constant height mode, the tip is held at a fixed distance (z) from the sample using a piezo ceramic element. By applying a voltage to this piezo, the tip is then raster-scanned across the sample, and the tunneling current is measured at a given number of x, y positions. The current is then plotted as a function of these positions. In constant-current mode, the tip is moved up and down (z direction) to maintain a fixed current (inputted by the microscope user) as the piezo scans the tip across the sample. The height is measured and plotted at each x, y position to yield a topographic map of the surface. In order to move the tip vertically to maintain a constant current according to eq 1, a feedback loop is employed. This loop consists of an iterative process in which the electron tunneling current at a given x, y, z position is measured and compared to the desired setpoint current; the z position of the tip is then readjusted according to a form of eq 1 in order to equalize the setpoint and measured currents.

Electron tunneling is a quantum mechanical phenomenon that occurs even though the tip and the substrate are not in actual contact (Fig. 2). For a metal–vacuum–metal system, electrons of the tip, for instance, may tunnel out of filled states Ψ_t, through a potential barrier of height U and width d, and into unfilled states of the substrate Ψ_s. The tunneling current is proportional to the coupling between Ψ_t and Ψ_s squared ($I \approx |\langle\Psi_t|\mathcal{H}|\Psi_s\rangle|^2$, where $\mathcal{H}$ is a Hamiltonian operator).

Initial STM experiments provided remarkable images of bare metal and semiconductor surfaces; these types of experiments confirmed the structures of a number of surfaces, including Au (*5, 6*) and Si (*7–9*). Studies such as these were conducted in clean ultrahigh vacuum environments to insure that few contaminants contributed to the STM images.

More recent investigations have been undertaken under ambient conditions at the liquid–solid interface. In these experiments, surfaces are covered with solutions comprising long-chain hydrocarbons that readily adsorb onto materials such as graphite and MoS_2 (*10–20*). By systematically varying the end group in a family of all-trans alkanes, ordering resulting from adsorbate–adsorbate and adsorbate–substrate interactions has been determined (*19*). Further, certain functional groups appear with greater contrast enhancement

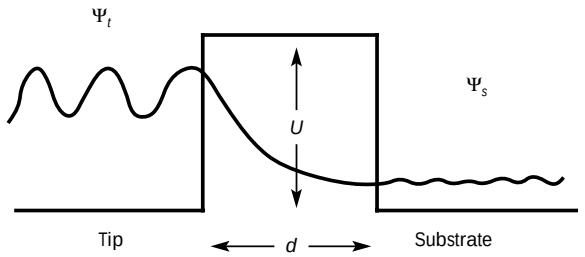

$$I \sim |\langle\Psi_t|\mathbf{H}|\Psi_t\rangle|^2$$

Figure 2. Quantum mechanical depiction of tunneling from tip states through a potential barrier and into substrate states. The barrier possesses a height U and a width d. The tunneling current is proportional to the coupling between the tip and substrate wave functions squared.

(brighter spots in the STM images) than the rest of the hydrocarbon chain. In constant-current mode, "bright" spots correspond to topographically higher regions (protrusions), while "dark" ones correlate with lower areas (depressions). The increased brightness can be attributed to a combination of geometric–topographic (e.g., size) and electronic coupling effects. A simple model proposed to describe the ability of STM to distinguish chemical functional groups correlates increasing functional group brightness with increasing molecular polarizability (*10, 11*). Based upon this correlation, the bromine atom in halogenated docosane ($C_{22}H_{45}$–X), for instance, would be expected to appear "brighter" than Cl but "darker" than I. Moreover, the topographic images obtained for these substituted molecules frequently reflect the shapes of their highest occupied and lowest unoccupied molecular orbitals (HOMOs and LUMOs, respectively) (*12, 21, 22*).

Experimental Method

In this hands-on laboratory undergraduate students obtained atomic and molecular photographs (i.e., topographic images) of an atomically flat, layered substrate, graphite, and then studied this surface when it was covered with phenyloctane solution containing 11-bromoundecanol. The instrument used was a Nanoscope III STM (Digital Instruments) with the "A" scanner (maximum scan size 700×700 nm^2). Furthermore, by collecting high resolution images and comparing them to images reported in the literature (*10–20, 23–26*), students were able to identify the bromide and hydroxyl parts of the molecular adsorbates. Using the Spartan molecular modeling program, they then constructed the frontier molecular orbitals for a similar molecule, 5-bromopentanol, and compared the calculated HOMOs and LUMOs to the STM images. Since 5-bromopentanol itself has a short chain length, it is not expected to have a large enough heat of adsorption at room temperature to physisorb at the graphite liquid–solid interface long enough to make STM imaging of this molecule possible (*27, 28*).

Tip Preparation

Using a pair of wire cutters, a piece of Pt/Rh wire (87/13) 0.25 mm in diameter is cut to a length of approximately 1.5 cm. With the cutters held horizontally and the flat side of the blades directed upward, the 1.5-cm length of wire is "snipped" to produce a sharp end. In principle, this end contains a single "tip" atom through which electron tunneling will occur. Caution must be exercised in handling this newly fabricated STM probe, since contact between the terminal "atom" and any surface will flatten the tip and impede the achievement of atomic resolution. Using a pair of tweezers, the tip is carefully inserted into the tip-holder mounted onto the cylindrical piezoelectric scanner. (For the Digital Instruments Nanoscope III STM scanner, the piezoelectric tube is located at the center of the scan head as shown in Figure 3a.)

Substrate Preparation

A piece of highly oriented pyrolytic graphite (dimensions of 1.2×1.2 cm, height approximately 0.1 cm) is cleaved to obtain a new, clean surface by applying a piece of tape to the top of the graphite and carefully peeling off the topmost layer. (ZYB monochromator-grade graphite was used in these

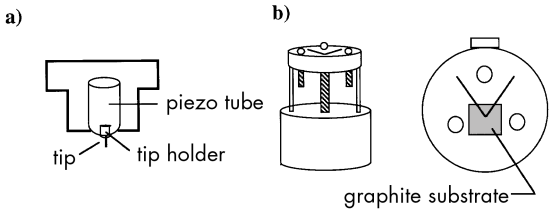

Figure 3. Schematic representations of the STM microscope used by physical chemistry undergraduate students. The cut-away view of the scan head (a) depicts a cylindrical piezo ceramic tube to which a tip-holder is affixed. A tip is seen protruding from the holder. Both side view (left) and top view (right) are shown for the STM base in (b). The three micrometer screws, responsible for coarse tip-sample approach, are visible, as is the v-shaped clip that holds the sample in place and delivers the bias voltage to the surface. The rear micrometer screw is connected to a stepper motor via a long shaft.

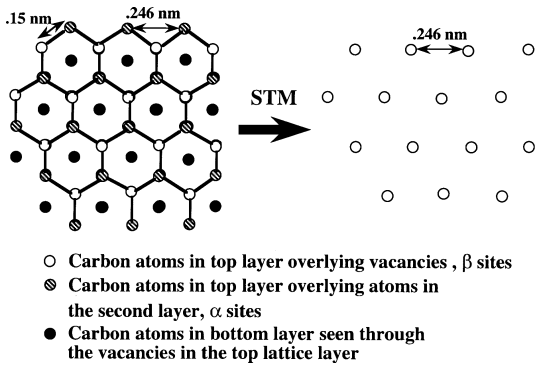

Figure 4. Representation of the graphite surface. Two layers are shown. One layer contains the electronically inequivalent α and β sites described in the text. The STM images carbon atoms in only one of these two sites in the top layer, as shown at right for the arbitrarily chosen atoms in the β sites.

experiments, although lower-grade pieces would likely work as well.) Tweezers or the edge of the tape can be utilized to remove any fragments that protrude from the graphite surface; these fragments can add to mechanical instability during scanning, resulting in noisy STM images. For the Nanoscope III, the substrate is mounted between the front two micrometer screws on the microscope base as shown in Figure 3b, making certain that nothing touches the graphite surface to be scanned. (There are a total of three micrometer screws on the microscope base. The front two are manually adjusted and the rear screw, while still manually adjustable, is attached to a stepper-motor.) A v-shaped clip, which is inserted into the base behind the front two micrometer screws, serves two purposes: first, it holds the substrate (graphite) in place, and second, it helps to apply the bias voltage to the sample.

Microscope Setup

The scanner is kinematically mounted on the micrometers. An optical microscope is used to locate the tip and the graphite substrate. The tip (which should appear with a pointed end) must be carefully lowered, using the micrometer adjustments, into proximity with the substrate by bringing the actual tip (extending downward) and its reflection (projecting upward) close together while avoiding contact. In doing so, the scan head should be made as horizontal as possible to reduce lateral and vertical piezo drift and STM equilibration time induced by head tilt. The STM is covered to reduce air currents, which add to image noise. Also, the microscope is placed on a bungee swing supported by an air table, which provides vibration isolation, necessary to reduce noise lines and attain atomic resolution.

While the physical chemistry students performed this laboratory exercise using the Digital Instruments microscope, the experimental procedure can be readily modified to be used in conjunction with a number of commercially available or home-built instruments. In addition, a concrete block suspended by bungee cords from a tripod or a spring-loaded platform set on top of a small granite slab can be substituted for the air-table and bungee-cord swing described above. In fact, two groups of students used the latter apparatus and were able to obtain atomic and molecularly resolved images.

Scanning Graphite (Atomic Photography)

To image clean metallic surfaces, a small bias voltage (typically 50–100 mV) and a large current (1–1.5 nA) are used. These tunneling parameters permit the tip to be positioned very close to the sample (recall eq 1). Since, as indicated below, the lattice spacing for graphite is small, a scan area of approximately 5×5 nm^2 best demonstrates the atomic resolution attainable for this surface. Owing to the drift that is observable on this scale, faster scan rates (typically 60 Hz) are necessary to minimize this effect.

After the STM scanning is begun, a real-time image of graphite is displayed. Graphite is a semimetal with a 0.246-nm lattice constant (*29*). As shown in Figure 4, the carbon atoms of graphite are arranged in a planar hexagonal sheet so that the distance between neighboring atoms is approximately 0.15 nm. The next hexagonal carbon sheet lies 0.335 nm below the first and is displaced in such a manner that three of the six carbon atoms in one hexagon reside directly over the carbon atoms of the underlying layer (α sites) and the other three lie over the vacancies (β sites). The STM will only image the topmost atoms in either the α or β positions. Bright spots corresponding to these carbon atoms spaced by 0.246 nm are shown on the STM monitor. If the spots are elongated as the STM scans in one direction (e.g., top to bottom) and compressed in the other, the STM is not equilibrated. (Causes for lack of equilibration include thermal drift of the sample and relaxation of the tip in its holder.) Equilibration for the Nanoscope III may take up to 20 minutes. Images devoid of spots and depicting noisy scan lines may reflect a poor tip. "Pulsing" the tip may help to improve resolution by picking up or releasing one or more surface- or tip-contaminating atoms. This can be accomplished by applying a large voltage (1.0 V) to the sample and then quickly reducing this voltage to the original bias value. This may be attempted several times in succession. (Voltage pulses above 2.0 V must be avoided, as these may cause the tip to break down the air, destroying both the tip and the sample.) If the STM image does not improve, a new tip will likely need to be cut. Assuming that the image looks promising, the distance between spots can be measured either in real time or in an off-line analysis routine. A nice-looking image (as shown in Fig. 5a) may be

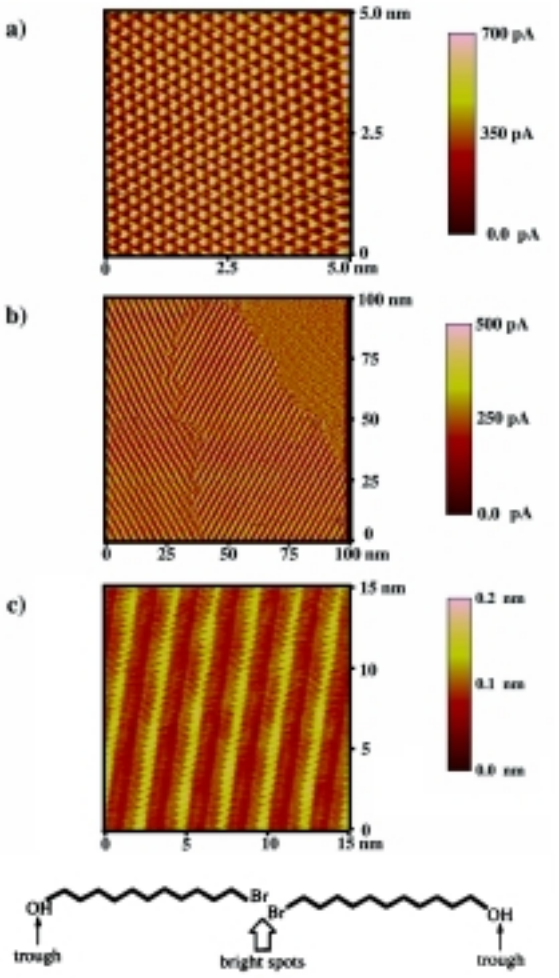

Figure 5. STM images obtained by physical chemistry students. A height scale corresponding to the color scale used in the images is shown to the right of each topograph. (a) 5×5-nm^2 scan of a bare graphite surface collected at 100 mV bias and 1.5 nA setpoint current. The bright spots in this constant-height image correspond to the locations of the inequivalent graphite lattice sites as described in Fig. 4. If this image of graphite reflected the positions of individual atoms, one might expect a pattern of spots separated by 1.42 Å, the carbon–carbon spacing. Instead, the spots are separated by ca. 2.5 Å, owing to the mapping of the density of states of two carbon sites. (b) 100×100-nm^2 scan of 11-bromoundecanol in phenyloctane solution physisorbed on a graphite substrate. The linear-appearing features are rows of individual molecules called lamellae. This image reveals two molecular domains. The scanning parameters were 1.5 V bias and 300 pA setpoint current for this constant-height image. (c) 15×15-nm^2 scan of 11-bromoundecanol physisorbed on graphite. This constant-current topograph was collected at –1.5 V and 300 pA setpoint current. The bright areas (greater tunneling probability) are attributed to the location of the Br functional group; the dark troughs represent the positions of the hydrogen-bonded hydroxyl groups. Six lamellae are displayed, each comprising two 11-bromoundecanol molecules. From left to right in one lamella, one sees the dark trough ascribed to the location of the hydrogen-bonding OH groups, the hydrocarbon backbone of the first molecule, and a bright spot corresponding to the positions of the bromine atom of the first molecule and that of its neighbor, then the hydrocarbon chain of the neighbor and its OH group in the second dark trough. This is shown schematically for two 11-bromoundecanol molecules of a single lamella below the STM image.

captured for students to submit as part of their laboratory reports. Students should be cautioned about talking or making loud noises while the STM topograph is being saved, since the STM is sensitive to vibrational and electronic as well as acoustic noise.

Scanning at the Liquid–Solid Interface (Molecular Photography)

The tip is now withdrawn to a position approximately 30 μm from the sample. The microscope can be uncovered and set upon a stable surface. A small amount (10 μL) of a 40 mg/mL solution of 11-bromoundecanol dissolved in phenyloctane is applied to the graphite substrate via a microsyringe, taking care not to hit the tip with the syringe needle. The solution spreads across the surface and creeps up along the tip by capillary action. The cover may be replaced and the STM carefully set on the bungee swing. The STM is reengaged using the same parameters employed above to scan the bare graphite surface in order to reconfirm the quality of the tip. To observe a monolayer of 11-bromoundecanol on the surface, the tip must be pulled slightly away from the substrate by changing the electron tunneling parameters. In general, a tunneling resistance (V/I) on the order of 10^9–10^{10} Ω is required for imaging molecular adsorbates. To accomplish this, the bias voltage is increased to approximately V_{bias} = |1.5 V| and the setpoint tunneling current is decreased to 300 pA. Since 11-bromoundecanol has a molecular length of approximately 1.3 nm, molecules are most easily seen (at least initially) for large 100×100 nm^2 scan sizes. When increasing the scan size, it should be remembered that slower scan rates (10–15 Hz) are best in order to avoid sweeping the physisorbed molecules from the surface. In addition, slightly larger feedback loop gain parameters are frequently required to procure clear STM images. If the molecules are not immediately apparent, the sign of the bias voltage may be switched, changing the direction of electron tunneling. Also, the molecules may be more stable on some areas of the surface than others, so moving to a new area can occasionally prove beneficial.

The physical chemistry students collected STM images for this large scan size in order to grasp the effects of long-range molecular order for these interfacial films. As seen in Figure 5b, one group of students observed multiple domains, presumably induced by a step edge on the graphite surface. Subtleties in the STM pictures such as these emphasize the effect of the surface on the molecular thin-film orientation. In addition, the long columns dominant in the image can be attributed to rows of individual molecules called lamellae. To see the molecules more clearly, smaller scan sizes are required. Images were captured for scan sizes ranging from 15×15 to 40×40 nm^2 in both constant-height and constant-current mode. The molecular axis for 11-bromoundecanol can be seen in a topograph such as that in Figure 5c. Here, the brighter spots (corresponding to greater tunneling) are attributed to the position of the bromide functionality, while the dark lines are ascribed to the location of the hydrogen-bonding OH groups. The students can measure the length of the lamellae and the angle between the lamella direction and molecular axis to learn about the structure of this molecular assembly.

11-Bromoundecanol is just one of the many molecules that can be studied as a physisorbed system on graphite in the undergraduate laboratory via STM. The literature contains numerous examples of molecules that may be used in a laboratory exercise (*10–13*, *15–20*, *23–26*).

Computational Analysis

The Spartan molecular modeling program is employed to calculate the frontier molecular orbitals (HOMO, LUMO, HOMO-1, and LUMO+1) for a brominated alcohol to compare to the collected STM images. The students ran this program on Silicon Graphics workstations. The students constructed an all-trans model of 5-bromopentanol using the "builder" window of the program and the tetrahedral carbon center, oxygen, and bromine atoms. Hydrogens appear on the molecule automatically. Calculation of the molecular orbitals was carried out using semiempirical methods on a geometrically optimized molecule. In the setup dialog box, the desired molecular orbital is chosen as a surface. This procedure is then repeated for the remaining three orbitals in order to add them to the same calculation. The actual calculation required less than three minutes. Students were asked to sketch the shapes of the orbitals to better compare them with their STM images and to consider which orbitals most resemble the molecular images. Figure 6 represents the molecular orbitals computed by one of the students for 5-bromopentanol, where the electron density is shown as dark and light gray clouds.

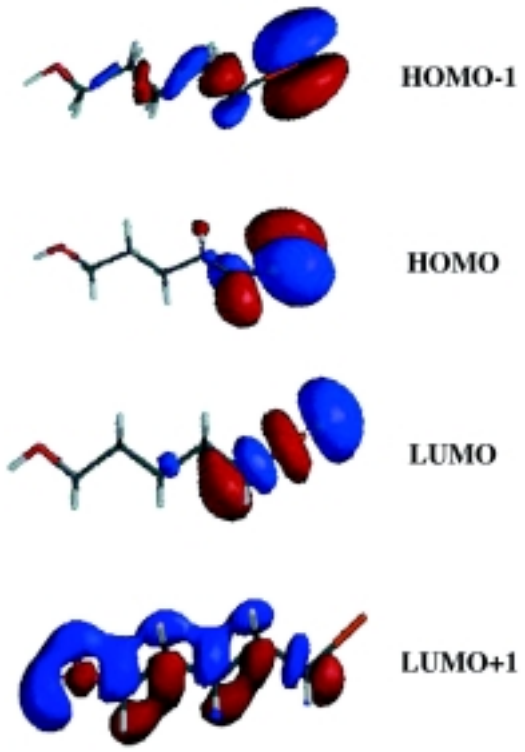

Figure 6. Frontier molecular orbitals of 5-bromopentanol calculated using the Spartan molecular modeling routine. Shown are the HOMO-1, HOMO, LUMO, and LUMO+1 orbitals. The dark and light gray regions represent areas where the wave function is localized. The bromine atom is located on the right side of the molecule and the hydroxyl group is positioned on the opposite end.

Results

For their laboratory reports, students were asked to discuss the operation of the STM, describe their collected STM images (they submitted three images with their reports: graphite, a 100×100 nm^2 scan of 11-bromoundecanol, and a small scan area of the molecular assembly), and compare the 11-bromoundecanol topographs with the molecular orbitals for 5-bromopentanol constructed using Spartan.

The undergraduate physical chemistry students were able to readily obtain good-quality STM images, as seen in Figure 5. In fact, the experiment, including a short introduction to the use of this specific microscope, was completed in less than three hours. The students performed the experiment with enthusiasm. The class as a whole seemed to grasp the major theoretical and experimental concepts of electron tunneling, as demonstrated by their laboratory write-ups. Many students searched the literature for more detailed descriptions of the theory and operation of the microscope. All of them correctly identified those molecular orbitals that contributed most to the STM images, correlating the localization of the wave function in the vicinity of the halogen atom with the increase in tunneling current exhibited in the collected STM images.

As a more quantitative measure of the educational benefit (from the physical chemistry student's perspective) of instituting STM experiments as part of the laboratory curriculum, the students completed a survey. The survey asked students about their feelings for the laboratory exercise and the knowledge they gained, and solicited constructive criticisms for improving the lab. The feedback was overwhelmingly positive. Students were enthusiastic and made comments such as "spectacular images". Their constructive criticisms of the handout stressed a desire for more information on the theory behind STM and what they felt were interesting experimental phenomena (e.g., contrast inversion observed in some graphite images). They unanimously agreed with the survey statements that the experiment was stimulating and informative, the technique used to collect images was straightforward, and the STM images gave a clear picture of molecular assembly ("like doing molecular photography"). Responses concerning the computational portion of the exercise were far more varied. Some students agreed that the combination of modeling and STM gives a critical sense of theoretical approximations learned in lecture (one stated "HOMO's and LUMO's are cool"), whereas others remarked that the relationship between the Spartan calculations and STM was difficult to understand.

Conclusions

The scanning tunneling microscope has been successfully introduced into the Columbia University physical chemistry laboratory curriculum. The laboratory investigation described above provides students with a stimulating hands-on experience in the use of this state-of-the-art surface analysis tool. Students were able to collect STM topographs both of a bare graphite surface and of 11-bromoundecanol physisorbed on

this surface, thereby suggesting the use of the STM as an atomic or molecular "camera". Moreover, calculation of the shapes of the frontier molecular orbitals of a structurally similar brominated alcohol emphasizes that areas of high tunneling current reflect regions of greater electron density of states and not just the position of individual atoms. Thus, this investigation demonstrates to students the productive coupling of experimental measurements with theoretical calculations.

Future developments for this laboratory will include imaging a series of molecules to give students a sense of how molecular assembly changes as a result of molecule–molecule interactions such as hydrogen bonding. In addition, studies on brominated alcohols, carboxylic acids, alkanes, and a non-brominated molecule (e.g., *n*-alcohol) will provide more concrete examples of the link between molecular orbital calculations and the influence of the electron density of states in STM imaging.

Acknowledgments

We would like to thank the physical chemistry students, Jackson Cheung, Rachel Ching, Ibrahim Daaro, Nathan Fishkin, Naomi Goldberg, Michael McLaughlin, Jenny Ramirez, Seth Rubin, Richard Urman, and Zachary Weinberg. In addition, we express our gratitude to Dalia Yablon for testing the experimental method prior to its application in the undergraduate laboratory. Equipment used in these experiments is part of Columbia's STM Research Facility, which is supported by the National Science Foundation (DMR-94-24296 and CHE-97-27205) and by the Joint Services Electronics Program (U.S. Army, Navy, and Air Force; DAAG55-97-1-0166).

Literature Cited

1. Coury, L. A.; Johnson, M.; Murphy, T. J. *J. Chem. Educ.* 1995, *72*, 1088.
2. Rapp, C. S. *J. Chem. Educ.* 1997, *74*, 1087–1089.
3. Binnig, G.; Rohrer, H.; Gerber, C.; Weibel, E. *Phys. Rev. Lett.* 1982, *49*, 57-60.
4. Strausser, Y. E.; Heaton, M. G. *Am. Lab.* 1994, 1–7.
5. Hallmark, V. M.; Chiang, S.; Rabolt, J. F.; Swalen, J. D.; Wilson, R. J. *Phys. Rev. Lett.* 1987, *59*, 2879–2882.
6. Woll, C.; Chiang, S.; Wilson, R. J.; Lippel, P. H. *Phys. Rev. B* 1989, *39*, 7988–7991.
7. Binnig, G.; Rohrer, H. *Surf. Sci.* 1985, *152/153*, 17–26.
8. Hamers, R. *Annu. Rev. Phys. Chem.* 1989, *40*, 531–559.
9. Tromp, R. M.; Hamers, R. J.; Demuth, J. E. *Phys. Rev. B* 1986, *34*, 1388–1391.
10. Cyr, D. M.; Venkataraman, B.; Flynn, G. W.; Black, A.; Whitesides, G. M. *J. Phys. Chem.* 1996, *100*, 13747–13759.
11. Cyr, D. M.; Venkataraman, B.; Flynn, G. W. *Chem. Mater.* 1996, *8*, 1600–1615.
12. Ikai, A. *Surf. Sci. Rep.* 1996, *26*, 261–332.
11. Cyr, D. M.; Venkataraman, B.; Flynn, G. W. *Chem. Mater.* 1996, *8*, 1600–1615.
12. Ikai, A. *Surf. Sci. Rep.* 1996, *26*, 261–332.
13. Claypool, C. L.; Faglioni, F.; Goddard, W. A.; Gray, H. B.; Lewis, N. S.; Marcus, R. A. *J. Phys. Chem. B* 1997, *101*, 5978–5995.
14. Cincotti, S.; Rabe, J. P. *Appl. Phys. Lett.* 1993, *62*, 3531–3533.
15. Rabe, J. P.; Buchholz, S. *Phys. Rev. Lett.* 1991, *66*, 2096–2099.
16. Rabe, J. P.; Buchholz, S. *Science* 1991, *253*, 424–427.
17. Rabe, J. P. *Ultramicroscopy* 1992, *42*, 41–54.
18. Rabe, J. P.; Buchholz, S.; Askadskaya, L. *Synth. Met. 1993*, *54*, 339–349.
19. Venkataraman, B.; Breen, J. J.; Flynn, G. W. *J. Phys. Chem.* 1995, *99*, 6608–6619.
20. Venkataraman, B.; Flynn, G. W.; Wilbur, J.; Folkers, J. P.; Whitesides, G. M. *J. Phys. Chem.* 1995, *99*, 8684–8689.
21. Hoshino, A.; Isoda, S.; Kurata, H.; Kobayashi, T. *J. Appl. Phys.* 1994, *76*, 4113–4120.
22. Takeuchi, H.; Kawauchi, S.; Ikai, A. *Jpn. J. Appl. Phys.* 1996, *35*, 3754–3758.
23. Giancarlo, L.; Cyr, D.; Muyskens, K.; Flynn, G. W. *Langmuir* 1998, *14*, 1465–1471.
24. Giancarlo, L. C.; Flynn, G. W. *Annu. Rev. Phys. Chem.* 1998, *49*, 297–336.
25. Fang, H.; Giancarlo, L. C.; Flynn, G. W. *J. Phys. Chem. B* 1998, *102*, 7421–7424.
26. Fang, H.; Giancarlo, L. C.; Flynn, G. W. *J. Phys. Chem. B* 1998, *102*, 7311–7315.
27. Findenegg, G. H. *J. Chem. Soc. Faraday Trans.* 1972, *68*, 1799.
28. Findenegg, G. H. *J. Chem. Soc. Faraday Trans.* 1973, *63*, 1069–1078.
29. Pisanty, A. *J. Chem. Educ.* 1991, *68*, 804–8088